

Figure 4.1

$C_m - \alpha$  curves for different tail settings (tail leading edge down is positive  $i_t$ ) showing trimming at different angles of attack.



Figure 4.2

All tail deflection on F-111. ([http://lh6.ggpht.com/\\_kIWY2DV0KnE/TPFmFd9fwbl/AAAAAAAAAIDE/WUnvwGvsbyg/F-111%20tail%20showing%20all-moving%20horizontal%20stabilizer.jpg](http://lh6.ggpht.com/_kIWY2DV0KnE/TPFmFd9fwbl/AAAAAAAAAIDE/WUnvwGvsbyg/F-111%20tail%20showing%20all-moving%20horizontal%20stabilizer.jpg))

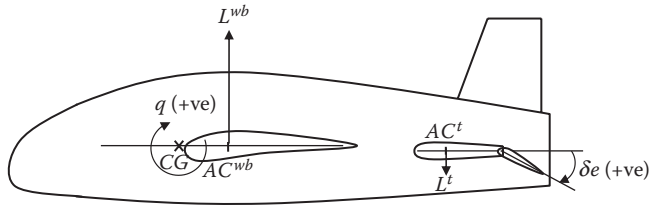


Figure 4.3  
Wing-body plus horizontal tail configuration with positive elevator (down) deflection.

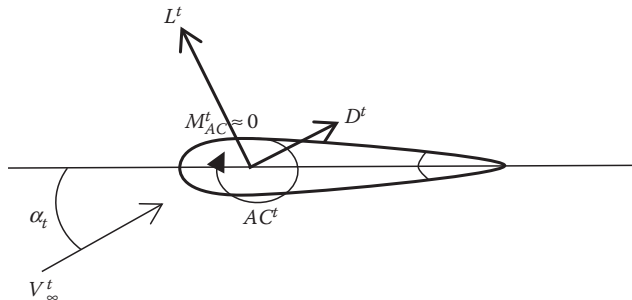


Figure 4.4  
Forces and moment at the tail at zero elevator deflection.

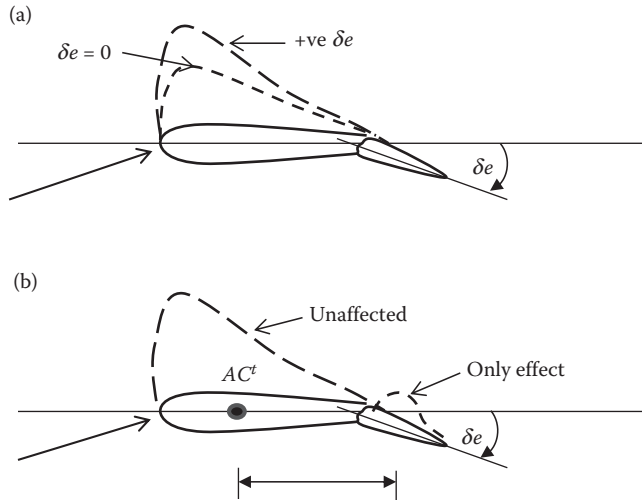


Figure 4.5  
Tail plus elevator combination in (a) subsonic and (b) supersonic flow.

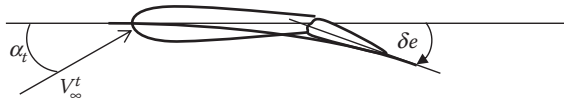


Figure 4.6

Tail at positive elevator deflection and equivalent camber line (shown thick).

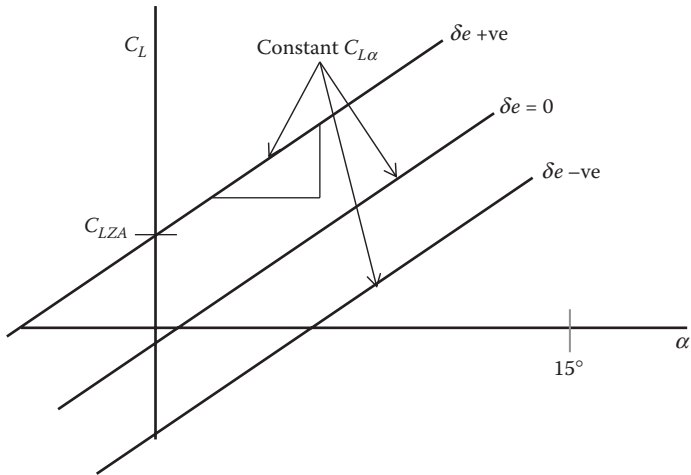


Figure 4.7  
 $C_L$  versus  $\alpha$  curves for different elevator deflections.

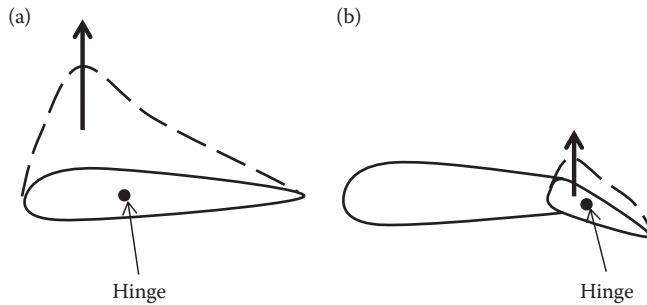


Figure 4.8  
(a) Tail hinge moment and (b) elevator hinge moment at tail.

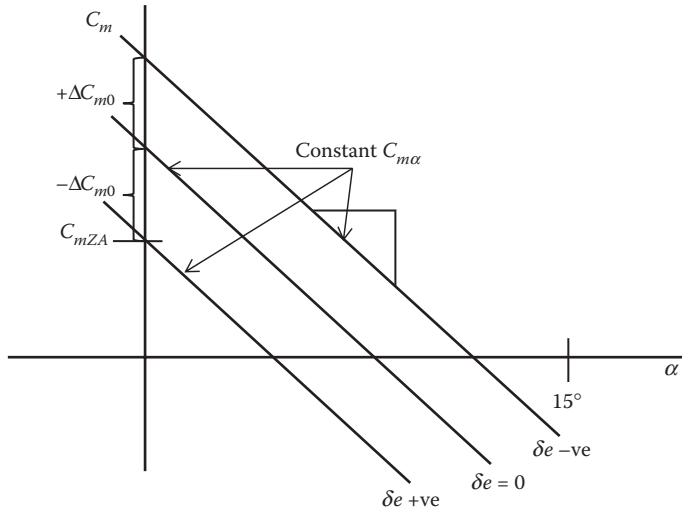


Figure 4.9  
 $C_m$  versus  $\alpha$  curves for different elevator deflections.

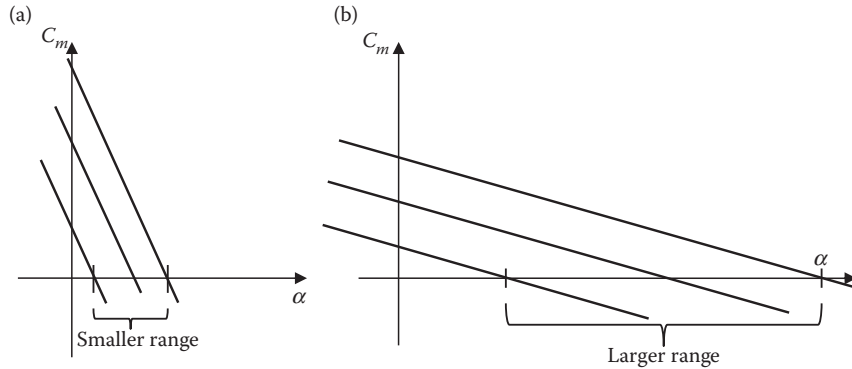


Figure 4.10  
 $C_m$  versus  $\alpha$  curves with different slopes, giving (a) smaller range and (b) larger range of trim  $\alpha^*$ .

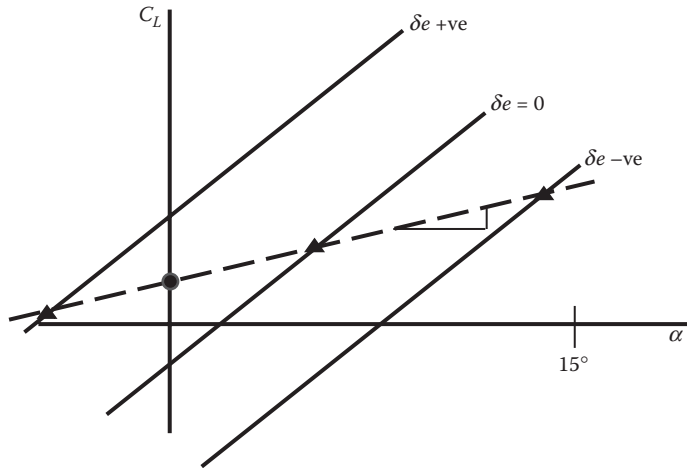


Figure 4.11  
(Solid line)  $C_L$  versus  $\alpha$  curves for different elevator deflections and (dashed line)  $C_L$  versus  $\alpha$  trim curve.

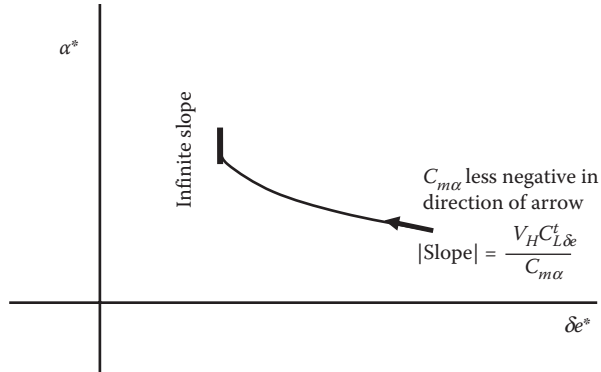


Figure 4.12  
Trim alpha versus elevator deflection.

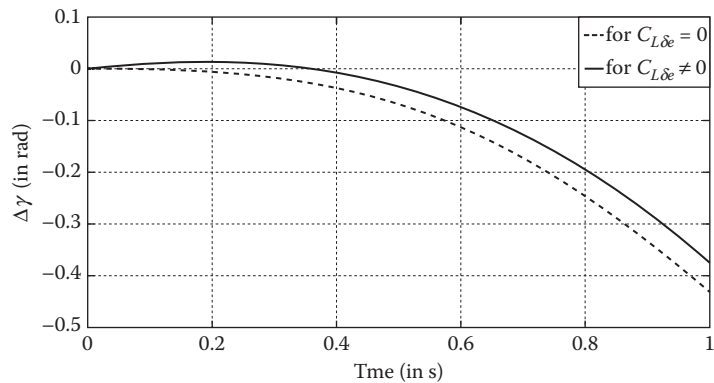


Figure 4.13  
Flight path angle  $\Delta\gamma$  response to a step elevator input (Equations 4.29 and 4.30).

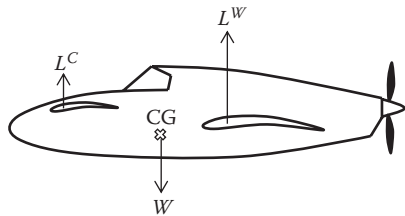


Figure 4.14  
A pusher-type airplane with canard.

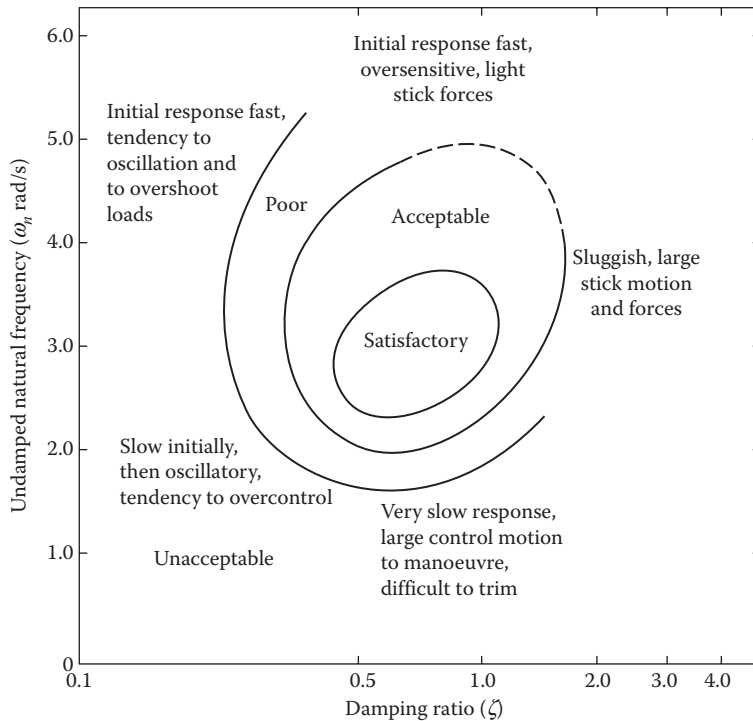


Figure 4.15  
Handling qualities criterion for short-period mode. (F. O'Hara. *Handling Criteria. J. Royal Aero. Soc.*, Vol. 71, No. 676, pp. 271–291, 1967.)

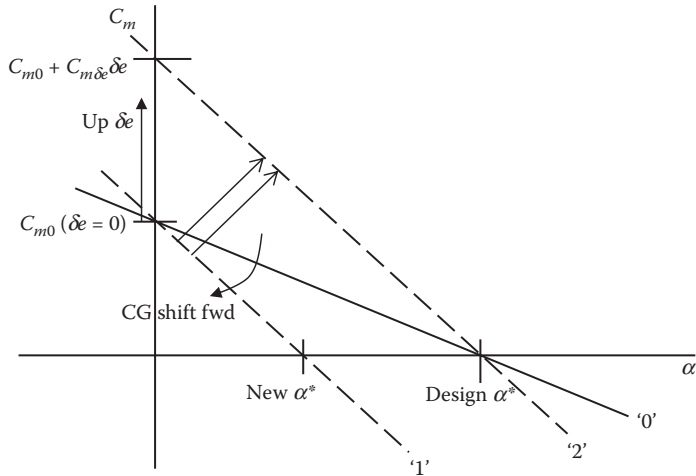


Figure 4.16  
Effect of CG shift and elevator deflection to recover trims.

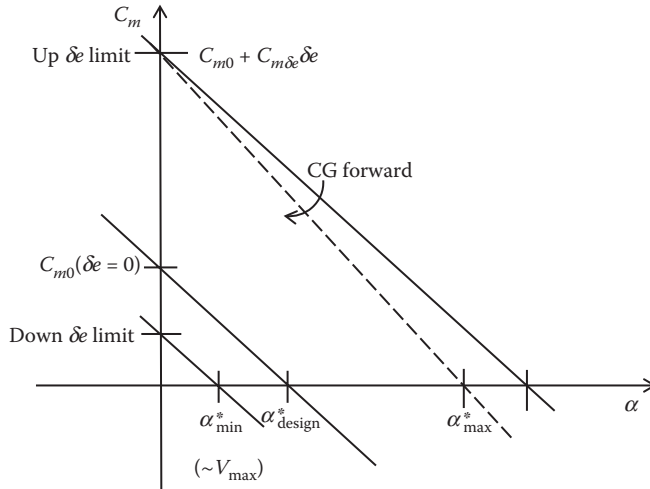


Figure 4.17  
Forward CG limit and elevator deflection limits.

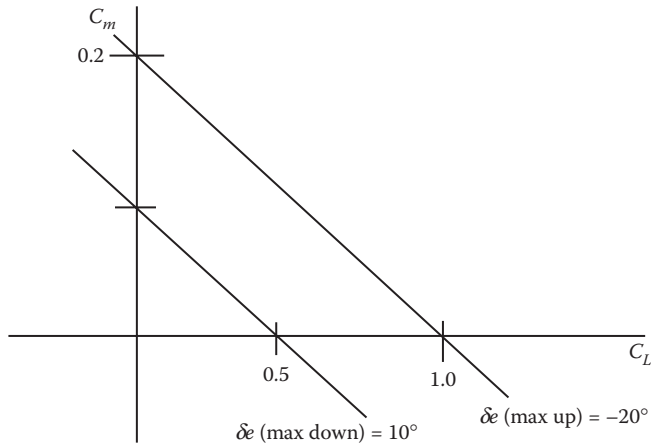


Figure 4.18  
 $C_m - C_L$  plot for maximum elevator deflections.

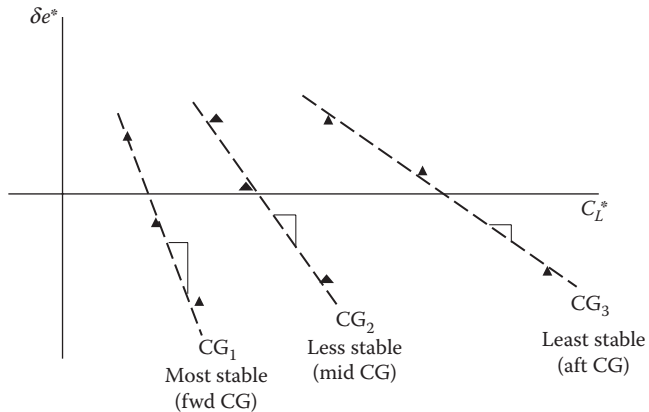


Figure 4.19  
Elevator required to trim versus trim lift coefficient for different CG locations.

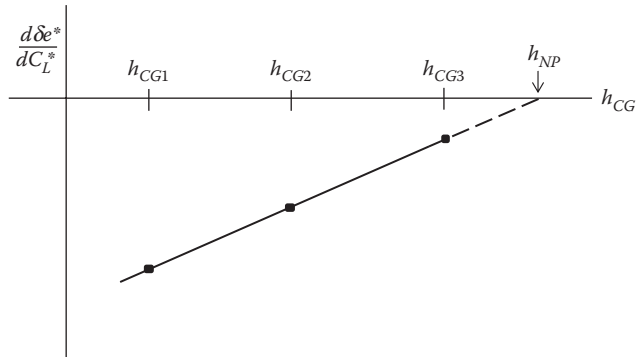


Figure 4.20  
Neutral point estimation from flight test.

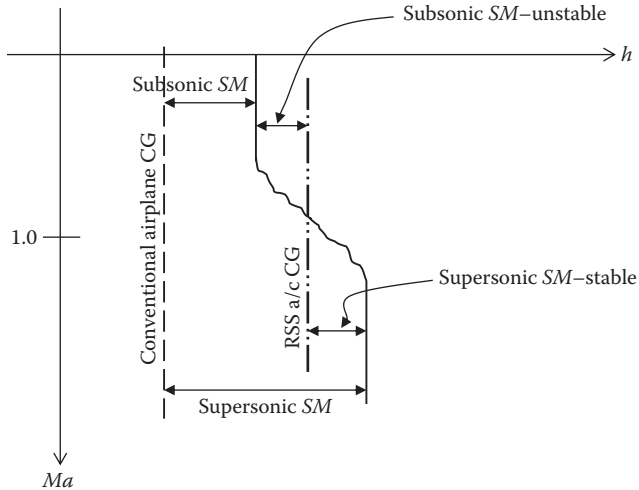


Figure 4.21  
Shift in neutral point with Mach number and CG management in conventional and relaxed static stability (RSS) airplanes.

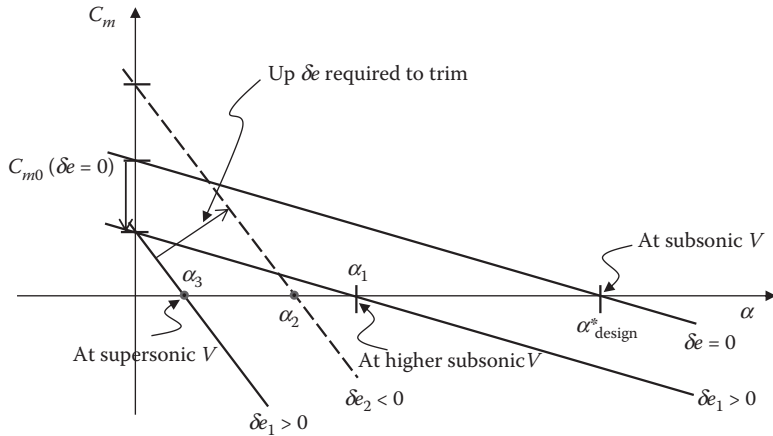


Figure 4.22  
 $C_m$  vs.  $\alpha$  curve for different flight speed conditions.

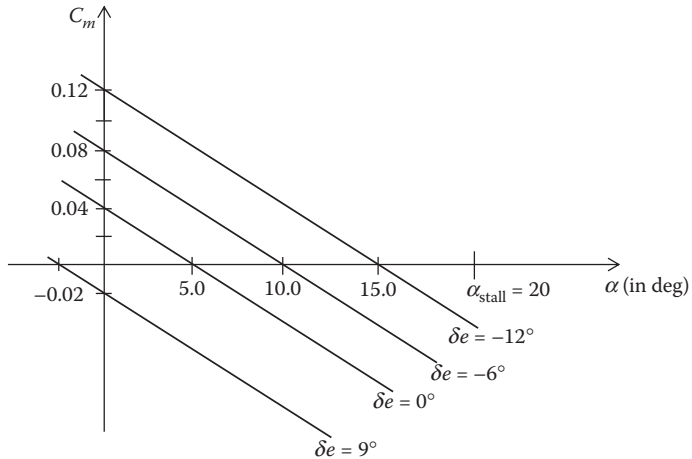


Figure 4.23  
 $C_m$  versus  $\alpha$  curves for different elevator deflections.